

Improvement of the filtration characteristics of calcite slurry by hydrocyclone classification

Vehmaanperä Paula, Safonov Dmitry, Kinnarinen Teemu, Häkkinen Antti

This is a Final draft version of a publication
published by Elsevier
in 10.1016/j.mineng.2018.08.042

DOI: DOI number of the original publication

Copyright of the original publication: © 2018 Elsevier Ltd.

Please cite the publication as follows:

Vehmaanperä, P., Safonov, D., Kinnarinen, T., Häkkinen, A. (2018). Improvement of the filtration characteristics of calcite slurry by hydrocyclone classification. Minerals Engineering, Volume 128. Pp. 133-140. DOI: 10.1016/j.mineng.2018.08.042

**This is a parallel published version of an original publication.
This version can differ from the original published article.**

Improvement of the filtration characteristics of calcite slurry by hydrocyclone classification

Paula Vehmaanperä*, Dmitry Safonov, Teemu Kinnarinen, Antti Häkkinen

LUT School of Engineering Science, Lappeenranta University of Technology,
P.O. Box 20, FI-53851 Lappeenranta, Finland

*Corresponding author: paula.vehmaanpera@lut.fi

Abstract

Hydrocyclones are used in the classification of solids for instance in the mining and minerals processing industries for modifying the particle size distribution of solids, as well as for ore concentration purposes. Improvement in the filtration properties of the slurry is usually achieved as a result of the classification process when only the underflow is evaluated, owing to the coarse and narrow particle size distribution. However, overall comparisons of the filtration properties incorporating filtration of both the underflow and overflow streams have not been discussed a lot in the literature. The objective of this study is to investigate hydrocyclone classification of a calcite slurry, to evaluate the resulting pressure filtration properties of the underflow and overflow streams, and to compare the required total filtration areas for a constant solids production capacity. The results show that the average specific cake resistance depended primarily on the fine particle content of the slurry, and therefore the Kozeny-Carman equation was not suitable for the prediction of the specific cake resistance. The specific resistances of feed and underflow filter cakes were underestimated consistently. Wide particle size distribution was one of the most apparent factors reducing cake porosity. The main outcome of the comparison of the required filtration areas was that a low specific cake resistance and high solids concentration of the underflow caused the total area requirement to decrease almost in all cases, compared to the area required for the filtration of the feed slurry. Moreover, as high as 99 % reduction in the total filtration area, compared to the feed slurry, could be achieved by filtering only the underflow streams, omitting the dewatering of the overflow streams. In the light of the promising results of the study, the incorporation of a classification step prior to filtration should be investigated further, e.g. in tailings treatment applications.

Keywords: Classification; Hydrocyclone; Filtration; Specific cake resistance; Particle size distribution

1. Introduction

Hydrocyclones are used for various classification purposes in the mining and minerals processing industries. Hydrocyclones are applicable in dividing the feed solids continuously into fine (overflow) and coarse (underflow) fractions, which opens great possibilities for their use for two main purposes: pretreatment of slurry prior to filtration, to enable cost-effective filtration of the coarse underflow fraction with vacuum filters, and concentrating the valuable components present in ores (Bradley, 1965, Rushton et al., 2000). Reaching the required classification result is difficult in many applications, and therefore hydrocyclones are often installed in circuits involving recirculation back to the grinding stage and/or the use of more than one classification step (Boylu, 2010; Yianatos et al., 2002).

The pressure filtration properties of slurries are affected by several particle properties, for instance the size and shape of the particles, the shape of the size distribution, and interactions between the liquid and the particles (Mota et al., 2003; Wakeman, 2007; Yu et al., 2017). Filtration can be made easier by a couple of methods based on changing the properties of the slurry. Pretreatment methods, such as slurry thickening, flocculation and particle classification are typically used in the mining and minerals processing industries (Anlauf and Sorrentino, 2004; Hogg, 2000; Rushton, 2000). When the feed slurry contains very fine particles, which make the filtration challenging, the use of flocculants may be the most realistic, although not very cost-effective, option to improve the filtration capacity. Moreover, flocculation requires the addition of chemicals in the process, which needs to be avoided in many cases. Regarding the solid-liquid separation step, hydrocyclones are especially useful in cases where the particle size distribution of the feed is wide. This is because hydrocyclone classification enables narrowing the particle size distribution and reducing the fines content of the slurry in a single separation step. It has been reported in the literature (e.g. Kinnarinen et al., 2017) that reduction of the width of the distribution to produce a more porous cake would facilitate the filtration in some cases, in spite of the reduction of particle size.

The aim of this experimental study is to investigate how classification of a calcite slurry by using a hydrocyclone would affect the filtration properties of the underflow and overflow streams, and to compare those results with the original slurry, with respect to the required filtration area for a constant amount of feed slurry processed. The average specific cake resistances and the average porosities of the cakes are correlated with particle size characteristics, and the applicability of the Kozeny-Carman relationship for predicting the specific cake resistance is discussed.

2. Theory and calculations

2.1. Hydrocyclone

Fig. 1 shows a schematic diagram of a hydrocyclone. Several different design variables have an influence on the performance of the hydrocyclone (Bradley, 1965; Cilliers, 2000). Table 1 presents the main variables and how they affect the cyclone performance. In Table 1, D_{50} is the cut size corresponding to the particle size which has 50 % probability to go to the underflow or the overflow, d_c is the diameter of the hydrocyclone, d_{VF} is the diameter of the vortex finder, d_{UF} is the diameter of the underflow spigot, h is the free vortex height, i.e. the distance from the bottom of the vortex finder to the top of the underflow spigot, and c_F is the volumetric solids concentration of the feed. The solids concentration of the feed slurry plays an important role in hydrocycloning. Increasing the solids concentration in the feed slurry increases the classification efficiency and the cut size D_{50} , but decreases the sharpness of the classification (Bradley, 1965; Cilliers, 2000; Lee, 2014). This effect is known as hindered settling, in which a higher number of particles moves outwards while the water flows towards the cyclone axis (Braun and Bohnet, 1990). The sharpness of the classification can be seen in the efficiency curve, which shows a percentage of a certain size of feed material that is recovered to the coarser underflow stream. A steep curve indicates sharp classification. Increasing the diameter of the vortex finder and the cyclone body increases the throughput volumes at a given pressure difference and the D_{50} values, as well as the sharpness of classification. The behavior of pressure drop is not so straightforward. An increase in the pressure drop increases the classification efficiency of the hydrocyclone and shifts the cut size D_{50} towards smaller

particles, but it does not automatically result in sharper or gradual classification. Furthermore, it seems that the rheology of the slurry does not have a significant effect on the throughput, water split and classification sharpness of the hydrocyclone, which suggests the use of a rheology modifier to be a favorable option to modify the cut size D_{50} (Tavares et al., 2002). On the other hand, Kawatra et al. (1996) report that the viscosity of the slurry has a significant effect on the classification. The changes in the solid concentration have been mentioned already, but the temperature and chemicals, among other factors, can also change the viscosity, and therefore change the cyclone performance (Cilliers et al., 2004; Kawatra et al., 1996). Despite the large number of influencing factors, computational fluid dynamics (CFD) and empirical modelling can be applied successfully in the performance evaluation of hydrocyclones (Cullivan et al., 2004; Hwang and Chou, 2017; Neesse et al., 2004a; Neesse et al., 2004b; Neesse and Dueck, 2007; Nowakowski et al. 2004; Schuetz et al., 2004).

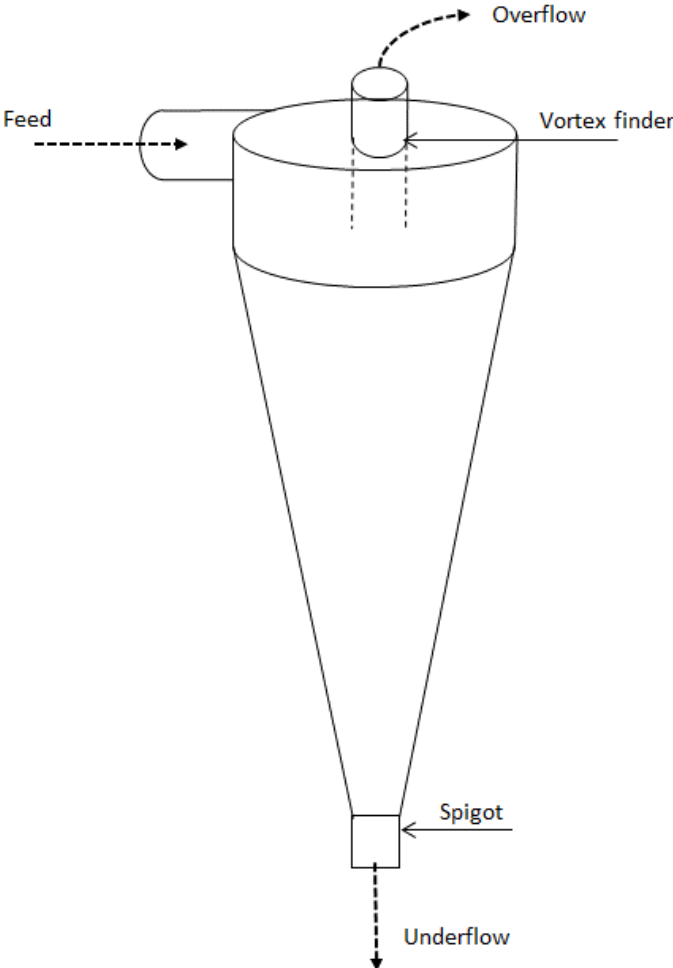


Fig. 1. Schematic diagram of a hydrocyclone.

Table 1 Influence of hydrocyclone parameters and operating variables on the result of classification. Plus signs indicate an increasing effect, whereas minus signs indicate a decreasing effect when the parameter or variable value is increased, according to Cilliers (2000).

Parameter*	Throughput	Cut size D_{50}	Classification sharpness
d_C	+	+	+
d_{VF}	+	+	+
d_{UF}	+	-	-
d_F	+	-	-
Cone angle	Not comparable	+	+
h	+	+	+
Pressure drop	+	-	+ or -
c_F	+	+	-

* d_C is the diameter of the cyclone, d_{VF} the diameter of the vortex finder, d_{UF} the diameter of the underflow spigot, d_F the diameter of the feed, h the free vortex height and c_F the volumetric solids concentration of the feed.

2.2. Pressure filtration

Cake filtration processes are greatly affected by the size of the solid particles, small particles being more difficult to separate than coarser ones (Kinnarinen et al., 2015; Wakeman, 2007). The particle mean diameter in filtration studies is usually defined on the basis of the surface area or volume. The Sauter mean diameter $D_{[3,2]}$ (m), i.e. the surface mean diameter, is defined as (Allen, 2003):

$$D_{[3,2]} = \frac{\sum_{i=1}^n D_i^3 v_i}{\sum_{i=1}^n D_i^2 v_i} \quad (1)$$

where D_i is the diameter of a particle (m) and v_i is the proportion of particles in the particle size fraction i .

Additionally, the volume mean diameter $D_{[4,3]}$ (m) is defined with the following equation:

$$D_{[4,3]} = \frac{\sum_{i=1}^n D_i^4 v_i}{\sum_{i=1}^n D_i^3 v_i} \quad (2)$$

The values for $D_{[3,2]}$ and $D_{[4,3]}$ can be obtained easily straight from volumetric particle size distribution measurements, and the Sauter mean diameter can be utilized in the calculation of the volume-based specific surface area for a single spherical particle with the following equation:

$$S_v = \frac{6}{D_{[3,2]}} \quad (3)$$

The average specific cake resistance for constant pressure filtration, α_{av} (m/kg), is based on Darcy's law (Darcy, 1856) and is calculated with the following integrated equation, Eq. (4):

$$\frac{t}{V_f} = \frac{\alpha_{av}\mu c}{2A^2\Delta p} V_f + \frac{\mu R_m}{A\Delta p} \quad (4)$$

where t is time (s), V_f is the volume of the filtrate (m^3), μ is the dynamic viscosity of the filtrate, c is the mass of the dry cake divided by the volume of the filtrate (kg/m^3), A is the filtration area (m^2), Δp is the applied filtration pressure (Pa), and R_m is the filter medium resistance (1/m). By plotting t/V_f as a function of the filtrate volume V_f , the average specific cake resistance and filter medium resistance can be calculated by using the slope and intercept of the line, respectively. As an example, Fig.(2) is shown to demonstrate the t/V_f - V_f plots for the filtration experiments when the diameters of the vortex finder and underflow spigot were 14 and 8 mm, respectively. The slope and the intercept can be denoted as a and b , respectively, hence, the equations for the filtration resistances are the following:

$$\alpha_{av} = \frac{2A^2\Delta p}{\mu c} a \quad (5)$$

$$R_m = \frac{A\Delta p}{\mu} b \quad (6)$$

The average porosity (i.e. the volumetric void fraction) of filter cakes, ϵ_{av} (-), is calculated based on the volume of voids in the cake and the volume of the cake as:

$$\epsilon_{av} = 1 - \frac{m_s}{\rho_s LA} \quad (7)$$

where m_s is the mass of dry cake (kg) and L is the thickness of the cake (m). Svarovsky et al. (2000) have reviewed Eqs. (4-7) extensively.

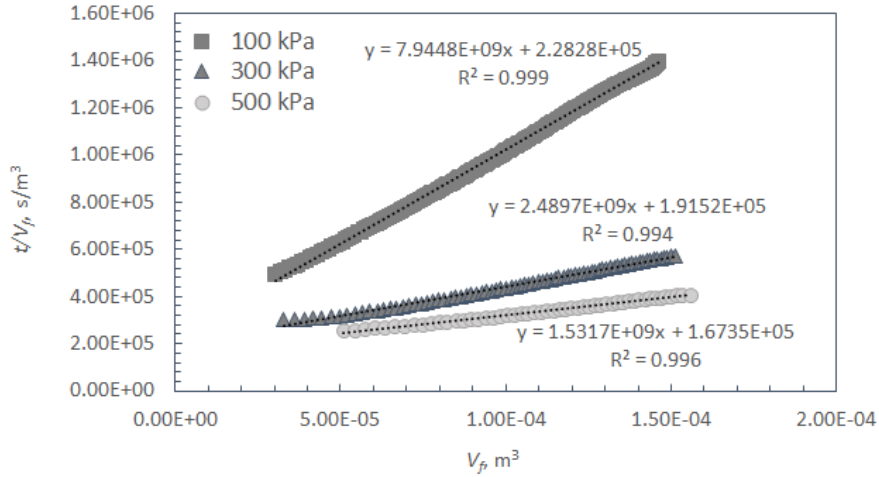


Fig. 2. An illustrative example of filtration data: linear graphs for calcite slurry obtained at three different filtration pressures.

The average specific cake resistance can be related to the porosity, the specific surface area and the density of solids by using Eq. (8), which is also known as the Kozeny-Carman equation (Rushton et al., 2000; Svarovsky, 2000).

$$\alpha_{av} = \frac{36K_0}{\rho_s(D_{[3,2]})^2} \frac{(1 - \varepsilon_{av})}{\varepsilon_{av}^3} \quad (8)$$

where K_0 is the Kozeny constant (-), which depends on the particle shape and surface properties and varies depending on the case. For example, $K_0=5$ is used in slow filtration, whereas $K_0=3.36$ in settling and rapid filtration. The typically used value $K_0 = 5$ (Rhodes, 2008) is used in this research. The Kozeny-Carman equation has been implemented widely in research (see eg. Besra et al. (2000)), but it is worth noting that the use of the Kozeny-Carman equation is limited, as it is valid only for narrow porosity ranges and incompressible cakes (Rushton et al., 2000; Svarovsky et al., 2000).

3. Materials and methods

3.1. Slurry preparation

The slurry was prepared from tap water and dried industrial ground calcium carbonate powder Parfill PF H 80 obtained from Nordkalk Oy (Parainen, Finland). The solid concentration of the slurry was constant 13.0 wt-% (5.1 vol-%) in all hydrocyclone experiments. The liquid density was 998 kg m⁻³ at the temperature of the experiments (19 °C). The characteristics of the feed slurry are presented in Table 2, where ρ_{sl} is the density of the slurry (kg m⁻³), C_s is the solid concentration (wt-%) and ρ_s is the density of the solids (kg m⁻³). The particle size distributions of the slurries were measured with a laser diffraction particle size analyzer (Malvern Mastersizer 3000 equipped with Hydro EV particle dispersing unit). All samples were measured five times by using the Fraunhofer optical model. The deviation between the measurements was under 1.0 %. The solids concentrations of all slurries were determined by drying a slurry sample at 105 °C for 24 h. The densities of the slurries were then calculated on the basis of the densities and masses of the solids and the liquid.

Table 2 Characteristics of the feed slurry. Subscripts *sl* and *s* represent the slurry and the solids, respectively

ρ_{sl} (kg m^{-3})	C_s (wt-%)	ρ_s (kg m^{-3})	D_{10} (μm)	$D_{[3,2]}$ (μm)	D_{50} (μm)	$D_{[4,3]}$ (μm)	D_{90} (μm)
1090	13	2756	2.09	5.72	22.3	37.1	93.0

3.2. Hydrocyclone experiments

The hydrocyclone experiments were carried out by using a MOZLEY c124 with a body diameter of 50.8 mm by varying the size of the vortex finder and the underflow spigot. The experimental setup is presented in Fig. 3. Table 3 presents the full factorial experimental design, showing the used combinations of the vortex finder (VF) and the underflow spigot (UF) diameters.

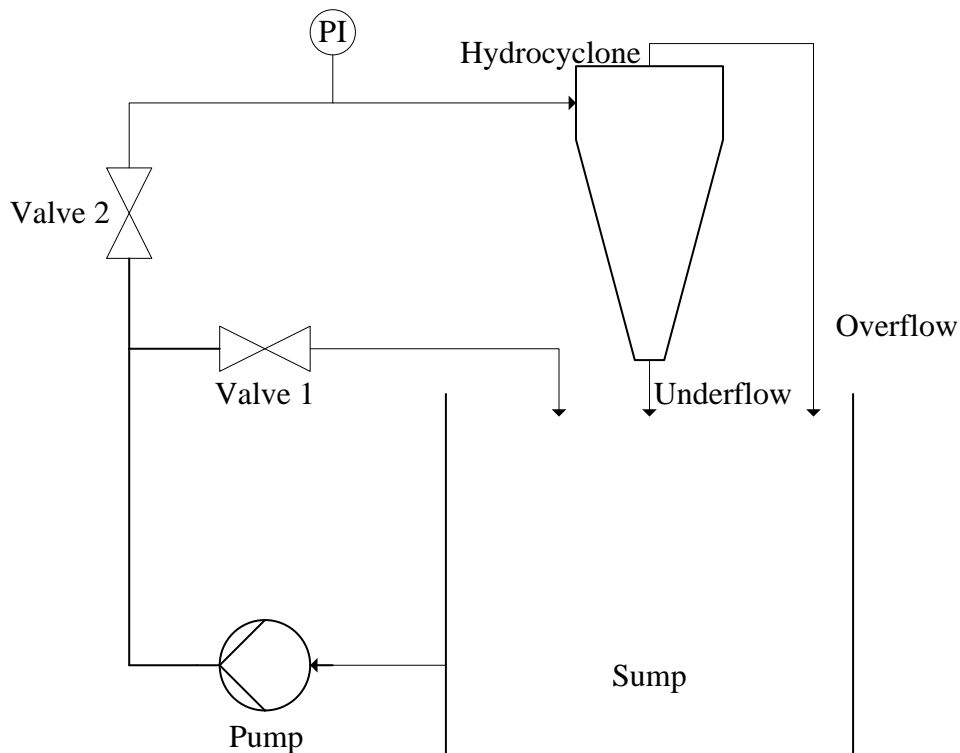


Fig. 3. Schematic diagram of the hydrocyclone system. The volume of the sump is 40 dm³.

Table 3 Experimental design for the hydrocyclone experiments. Subscripts *VF* and *UF* represent the vortex finder and the underflow, respectively

Experiment number (-)	d_{VF} (mm)	d_{UF} (mm)
1	14	3
2	14	5
3	14	8
4	11	5

5	8	3
6	8	5
7	8	8

First, the slurry was added to the sump and pumped through the system for 15 minutes to let the flow and the temperature stabilize. The feed pressure was adjusted to 150 kPa by using valves 1 and 2 (Fig. 3), and the same pressure was used in all experiments. The mass flow rates of the underflow and overflow were measured by the timed sampling method by using a container and a stopwatch, and a laboratory scale with the accuracy of 0.01g to measure the masses of the samples. The slurry samples were collected simultaneously from the underflow and overflow streams into separate containers. The particle size distributions were measured, the solid contents were determined, and the densities of the slurry samples were calculated as described above in Section 3.1. The remaining slurry samples were then used in the pressure filtration experiments.

3.3. Pressure filtration

All slurries, including the feed, underflows and overflows, were filtered with a Nutsche pressure filter at room temperature. The total volume of the cylindrical filter chamber was 350 cm³, and the chamber diameter was 52 mm. Pure cellulose discs (T-1000, Pall Corporation), used as filter media, were carefully wetted with deionized water prior to the filtration experiments. The mass of each batch of slurry was 300 ± 2 g, and the used pressure differences were 100, 300 and 500kPa. Additionally, filtration experiments were carried out twice at the filtration pressure of 300 kPa, so the total number of filtration experiments was 68. The feed slurry was filtered four times at three different pressures to be able to evaluate experimental error of the filtration experiments. The mass of the filtrate and the filtration pressure were recorded once a second with an automatic data collection system (LabVIEW by National Instruments, USA). The total filtration time was up to 30 min, depending on the slurry. After each experiment, the cake was dried to total dryness in an oven at the temperature of 105 °C to determine the moisture content.

4. Results and discussion

4.1. Properties of hydrocyclone streams

The influence of hydrocyclone parameters on particle characteristics is presented in Table 4. The results are fairly consistent, as the hydrocyclone was able to separate the particles into two clearly different particle populations: the coarser particles were found in the underflow, whereas the finer particles were found mainly in the overflow. The biggest changes were observed in the particle size distributions of the underflow samples, whereas the changes were not very remarkable in the case of the overflow. When the size of the vortex finder was a constant 14 mm and the size of the underflow spigot was increased from 3 to 8 mm, the particle size distributions of the underflow samples shifted clearly towards finer particle sizes, whereas smaller changes were observed in the overflow particle size distributions. The increase in the D_x values was more drastic for the underflow than for the overflow when the size of the vortex finder was increased from 8 to 14 mm, and the diameter of the underflow spigot was a constant 5 mm. These findings are in line with the findings made by Cilliers (2000).

Table 4 Particle size characteristics of underflow and overflow streams produced with different diameters of the vortex finder (VF) and the underflow (UF) opening

Dimensions		Underflow stream					Overflow stream				
d_{VF} (mm)	d_{UF} (mm)	D_{10} (μm)	$D_{[3,2]}$ (μm)	D_{50} (μm)	$D_{[4,3]}$ (μm)	D_{90} (μm)	D_{10} (μm)	$D_{[3,2]}$ (μm)	D_{50} (μm)	$D_{[4,3]}$ (μm)	D_{90} (μm)
14	3	14.6	16.2	44.7	57.4	114	1.09	2.68	4.89	7.67	16.90
14	5	9.54	12.6	35.4	48.1	103	1.00	2.33	3.72	5.97	12.10
14	8	3.88	8.04	28.2	39.8	91.3	0.98	2.21	3.32	5.63	11.50
11	5	6.06	9.6	29.5	40.5	92.7	0.93	2.02	2.91	4.09	8.16
8	3	7.12	10.5	30	42.2	94.4	0.95	2.09	3.06	4.67	8.54
8	5	3.95	8.21	30.8	46.1	109	0.94	2.02	2.81	4.42	7.93
8	8	2.11	5.98	25.1	41.8	106	0.90	1.85	2.36	4.58	9.18

Fig. 4 illustrates the particle size distribution of the feed slurry, overflow and underflow with the diameter of the vortex finder of 11 mm and underflow spigot of 5 mm.

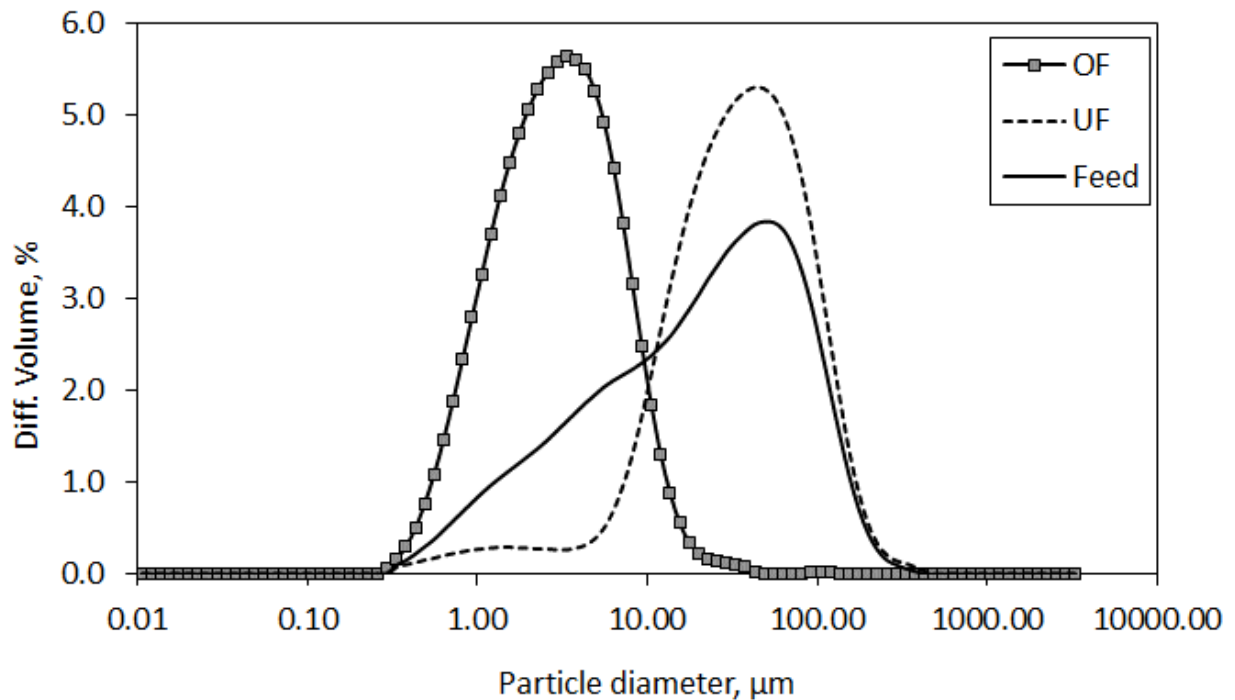


Fig. 4. Volumetric particle size distribution of streams when the diameter of the vortex finder and underflow spigot were 11 and 5 mm, respectively.

Table 5 shows the ratio between the underflow and overflow for solids and water in each test. As can be seen in Table 5, the variation in the ratio of solids between the underflow and

overflow was minor. The ratio was from 3:1 to 5:1 in all cases, with the exception of the underflow spigot of 8 mm and the vortex finder of 8 mm, when the ratio was 16:1. However, greater variation was observed in the ratios of water between the underflow and overflow. The overflow contained up to 20 times more water than the underflow in all the cases, excluding the experiment carried out with the 8 mm underflow spigot and 8 mm vortex finder. The solid concentration varied from 2.2 to 5.8 wt-% in the overflows and from 17.8 to 70.4 wt-% in the underflows. It can be clearly seen in Table 5 that using the same size of underflow spigot and vortex finder does not produce the desired classification result. Similar findings have been made by Ghadirian et al. (2015) and Gao et al. (2008). The latter also found that after a certain point, the increase in the diameter of the vortex finder did not automatically decrease the solids concentration in the overflow, which was explained by the increase in the residence time. According to Lee (2014), Pasquier and Cilliers, (2000) and Yu et al. (2017), increasing the diameter of the underflow spigot increases the underflow flow rate, which could be seen here as well. Taking into account the masses of solids and water, a similar trend was observed for the overflow, whereas the trend was naturally the contrary for the overflow. The classification efficiency E_T increased with the increase of the diameter of the underflow spigot and the decrease of the diameter of vortex finder, which was also observed by Pasquier and Cilliers (2000).

Table 5 The overflow (OF) and underflow (UF) mass ratios R_S and R_W for solids and water, respectively, and the dimensionless classification efficiency E_T . The solids contents C_s of the streams are also shown.

d_{VF} (mm)	d_{UF} (mm)	R_S (OF/UF) (-)	R_W (OF/UF) (-)	E_T (-)	C_s (UF) (wt-%)	C_s (OF) (wt-%)
14	3	0.44	17	0.69	68.5	5.4
14	5	0.43	21	0.70	70.4	4.6
14	8	0.41	4.3	0.71	39.4	5.8
11	5	0.32	11	0.76	57.2	3.9
8	3	0.35	15	0.74	63.6	4.0
8	5	0.21	3.4	0.83	35.2	3.2
8	8	0.06	0.6	0.94	17.8	2.2

4.2. Pressure filtration properties of the streams

The effect of particle characteristics on the filtration behavior was investigated by plotting the average specific cake resistance α_{av} against D_{10} , $D_{[3,2]}$, D_{50} and D_{90} (Fig. 5). As can be seen in Fig. 5, the results show a very clear correlation for most cases between particle size and average specific cake resistance. In the case of D_{10} values, the average specific cake resistance increased exponentially when the particle size decreased. The correlation seemed to shift towards linear correlation with the coarser particles, $D_{[3,2]}$, D_{50} , and D_{90} . $D_{[90]}$ values did not have a clear correlation with the average specific cake resistance in the case of underflow. Also Kinnarinen et al. (2015) have reported on a clear correlation between the particle size and the average specific resistance of filter cakes, and the fact that the data started to vary increasingly with the coarsest particle size fractions.

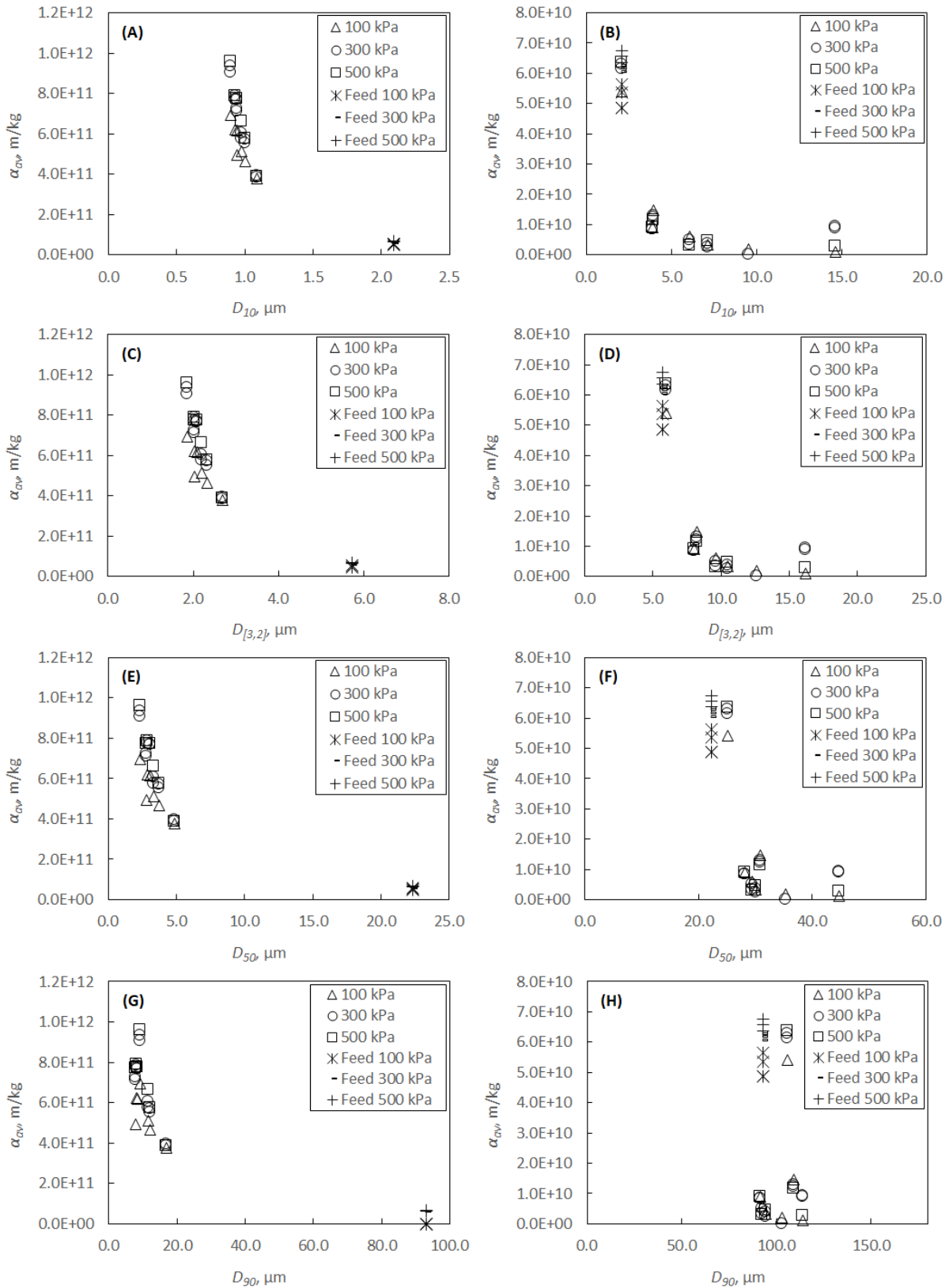


Fig. 5. Average specific cake resistance against different particle characteristics for the overflow (A, C, E, G) and the underflow (B, D, F, H).

The repeatability of the filtration experiments was evaluated by filtering the feed slurry four times at the pressures of 100, 300 and 500 kPa. Overall, the relative standard deviations of the

average specific cake resistance and the average porosity of the cake were observed to vary from 2 to 7 % and from 0.7 to 8 %, respectively. In the case of average specific cake resistance, the highest deviation was observed at the lowest filtration pressure (100 kPa), whereas no remarkable deviation was observed with the higher pressures (300 and 500 kPa). The lower the pressure the slower the cake formation during the filtration, which resulted in slight curvature the linear fits of the filtration data, V_f versus t/V_f , at the pressure of 100 kPa and, thus, bigger deviation in the determined filtration characteristics. In the case of the average porosity of the filter cakes, the smallest deviation was observed at the lowest filtration pressure and the highest deviation at the higher pressures. This may be explained by the uncertainty of the measurement of the thickness of the cake. The thickness of the thinnest cake was as low as 1mm, which is difficult to measure accurately, and can thus cause a large error in the average porosity. Therefore, these points have been left out from this study.

The effect of the width of particle size distribution is presented in Fig.6. Based on Fig.6, it seems that the width of particle size distribution, i.e. the span in this case, does have some correlation with the average porosity of the cakes. However, the trend of porosity against the span is slightly decreasing for the higher filtration pressures (300 and 500 kPa). Previous literature on the topic (Kinnarinen et al., 2015; Kinnarinen et al., 2017) shows clearer than the present results that a narrow particle size distribution usually results in higher cake porosities.

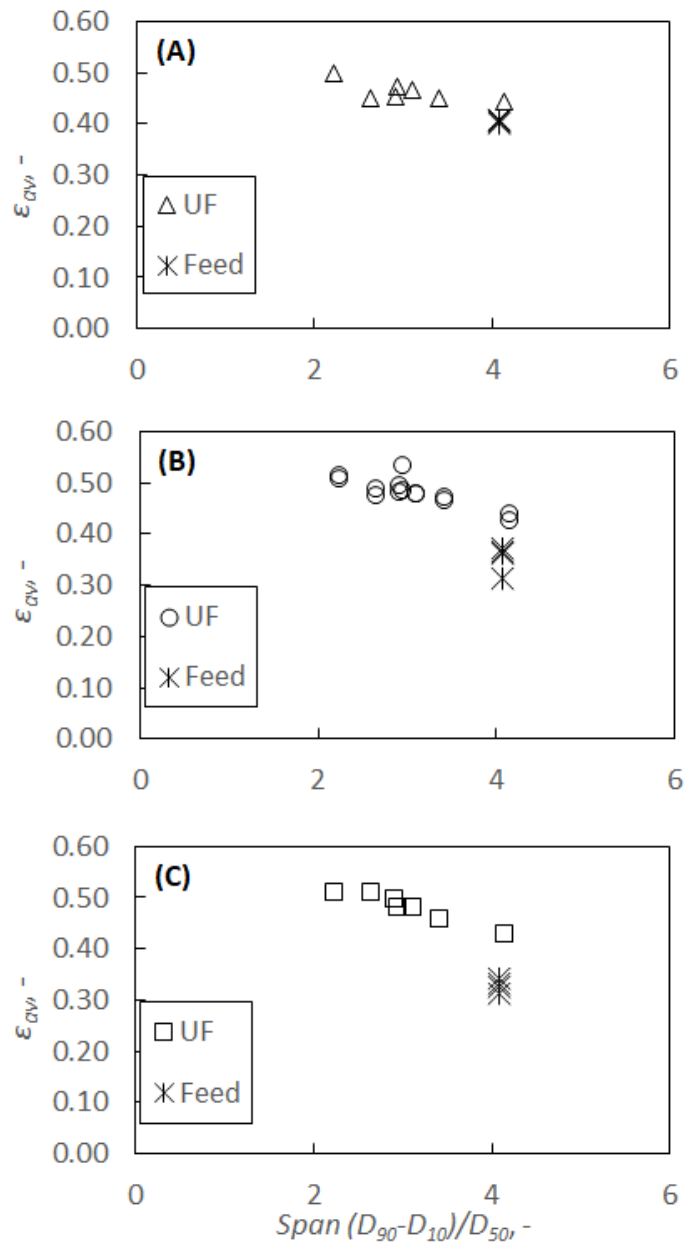


Fig.6. Average porosity of underflow and feed filter cakes against the width of particle size distribution at 100 kPa (A), 300 kPa (B), and 500 kPa (C).

Fig. 7 shows the correlation between the experimentally determined average specific cake resistance and calculated (Eq. (8)) values. It can be concluded clearly that the Kozeny-Carman equation was not applicable for the data. The equation underestimated the specific cake resistances in the case of underflow and feed. The authors argued that the reason might be the wide particle size distribution and the variation in the (non-spherical) shapes of particles (Besra et al, 2000). Moreover, the Kozeny constant K can vary, depending on the applied classification conditions, which causes uncertainty in the calculation of α_{av} values. In this study the wide particle size distribution was most probably not the reason for the poor predictability, as the slurries produced by hydrocyclone classification had narrow particle size distributions. The cakes were also slightly compressible, which might be the main reason for the poor applicability of the Kozeny-Carman equation, since the equation is not applicable for compressible cakes (Svarovsky, 2000). For instance, Tien and Ramarao (2013) also found the poor applicability of the Kozeny-Carman equation to the cake filtration data.

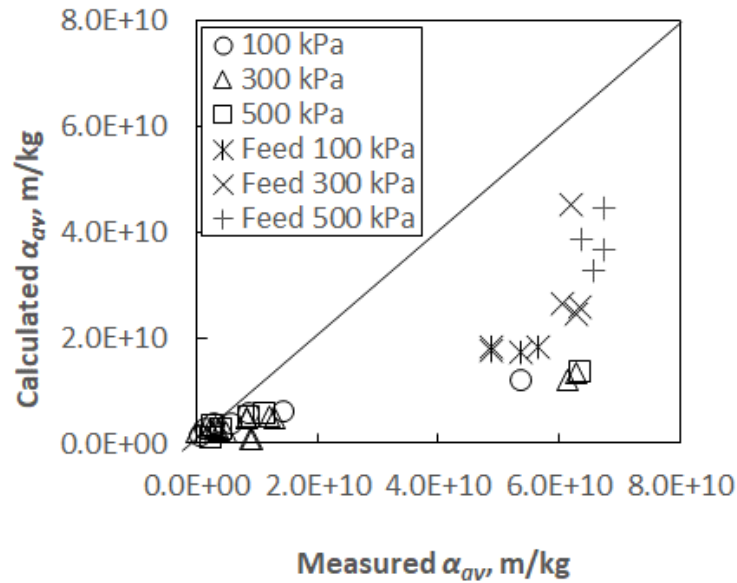


Fig.7. Measured versus calculated (Eq. (8)) average specific resistances of filter cakes for underflow. The solid line represents a 1:1 relationship.

Due to the poor ability of the Kozeny-Carman relationship to predict the specific cake resistance, the influence of the finest particles on the filtration behavior was investigated. As a result of an increase in the fraction of small particles, the average specific cake resistance showed linear behavior for the overflows (Fig.8A) and exponential behavior for the underflows (Fig.8B). These findings clearly support the fact mentioned above and also reported by Wakeman (2007): the smaller the particles, the more difficult the filtration. In the beginning of the cake filtration, the smallest particles may migrate through the filter medium and fill the voids in the formed cake, and thus form a skin layer close to the filter medium. Moreover, the smallest particles are the main reason for the increase in the specific surface area of the solid and the increased specific cake resistance.

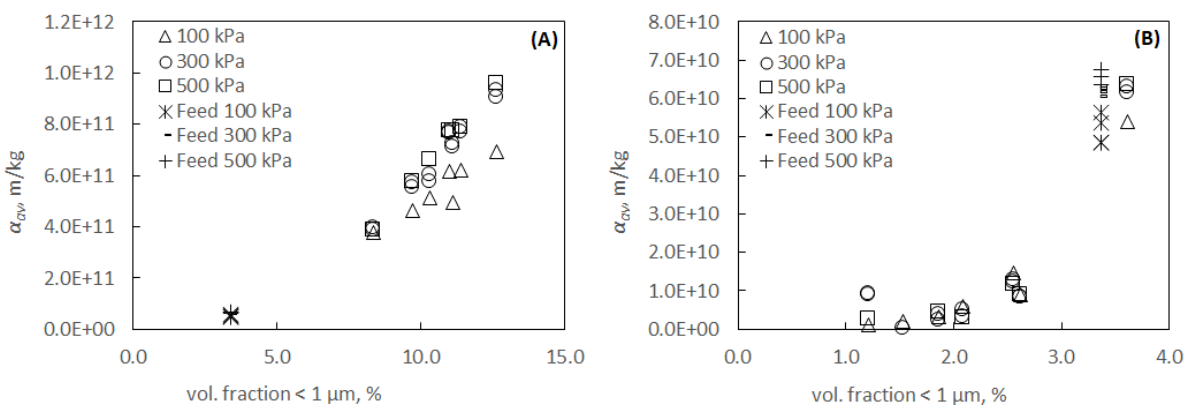


Fig. 8. Correlation between the average specific cake resistance and the volumetric fraction of particles smaller than one micron for the overflow (A) and underflow (B).

4.3. Scale-up and determination of required filtration area

The filtration area required to obtain an industrially relevant production capacity, 10 000 kg dry solids per hour, was calculated from Eq.(4) solved with respect to A , in order to evaluate whether hydrocyclone classification prior to filtration stage would be reasonable. The solids were assumed to be incompressible and the filtration was assumed to take place at a constant pressure. The technical time included in the operational cycle of industrial-scale pressure filters was omitted in the calculation. Two different scenarios were considered: 1) both the underflow and overflow streams are filtered, and 2) only the underflow streams are filtered and the overflow streams are not filtered. The first scenario represents a situation where all solids have to be recovered, while the second scenario represents a case where a compact filtration plant is preferred for the recovery of underflow only, and the overflow can be pumped to a pond. In some cases, the solids concentration of the overflow streams might be too low for the efficient cake filtration, and therefore there may be a need for other separation techniques, such as settling or centrifugation. Reduction in the filtration area was calculated by comparing the total area requirement ($A_{UF}+A_{OF}$) to the area requirement of the original feed slurry.

4.3.1. Both underflow and overflow filtered

The calculated areas (A_{UF} and A_{OF}) required for the filtration of the underflow (UF) and overflow (OF) streams are shown in Table 6. The reduction in the required filtration area obtained by hydrocyclone classification is also presented in Table 6. Clear differences can be observed between the underflow and overflow streams. The areas required for the filtration of overflows were up to 10-100 times larger than those for the underflows, but on the other hand, the areas did not differ much from the areas required for the filtration of the feed slurry. The most important reasons for these differences were the differences in the width of the particle size distributions (see Fig. 6 for cake porosity) and the solid concentration of the slurries. The total area needed for the filtration of underflow and overflow fractions was smaller than the area needed for the filtration of the original slurry. The superior filterability of the underflows was the most important factor explaining this result. The underflow slurries resulted in lower average specific cake resistances due to their larger particle size and high solids concentration. The total required filtration area with the vortex finder of 8mm and the underflow spigot of 8mm was the only case where the required area was higher than that for the feed slurry.

Table 6 Filtration area required to produce 10 000 kg dry solids/h. The required filtration areas for feed slurry were 32.2 and 26.4 m² at the filtration pressures of 300 and 500 kPa, respectively.

<u>Hydrocyclone dimensions</u>		<u>Filtration pressure and required filtration area</u>			<u>Reduction in the filtration area</u>
d_{VF} (mm)	d_{UF} (mm)	Δp (kPa)	A_{UF} (m ²)	A_{OF} (m ²)	R (%)
14	3	300	1.4	22.9	25
14	3	500	0.29	18.1	30
14	5	300	0.08	25.8	20
14	5	500	<0.01	20.7	22
14	8	300	6.3	25.3	2
14	8	500	5.2	20.8	2
11	5	300	2.9	24.3	16

11	5	500	2.1	19.0	20
8	3	300	2.0	24.9	17
8	3	500	1.9	19.7	18
8	5	300	9.7	16.0	20
8	5	500	7.4	13.3	22
8	8	300	29.5	6.2	-11
8	8	500	23.6	5.0	-8

4.3.2. Only underflow filtered

The second scenario was that only the underflow streams were filtered and the overflow streams were pumped to the tailings pond. The filtration areas, as well as the reduction in the required filtration areas, and the total separation efficiencies, are shown in Table 7, where a substantial reduction in the filtration area can be seen. In the best case, with the vortex finder of 14 mm and the underflow spigot of 5mm, the reduction was 99 %. Moreover, even in the least favorable case, with the vortex finder of 8mm and the underflow spigot of 8mm, the filtration area was reduced by 2 %. These results show clearly that classification with the hydrocyclone plays an important role in improving the filtration process. Moreover, from the economic point of view, in applications where the valuable metals are concentrated more to the coarse fraction, it may be reasonable to filter only the underflow. In some cases, the hydrocyclone can classify the hazardous metals (such as Cd, Pb, Ni and Zn) to the finer particle size fraction, whereas the valuable compounds stay in the underflow streams, which makes the filtration only the underflow streams attractive, as demonstrated with success by Golmaei et al. (2018).

Table 7 Filtration area of underflow streams required to produce 10 000kg dry solids/h. The reduction in the filtration area R and the dimensionless total classification efficiency E_T are also shown.

<u>Hydrocyclone dimensions</u>		<u>Filtration pressure and required filtration area</u>		<u>Reduction in the filtration area</u>	<u>Total separation efficiency</u>
d_{VF} (mm)	d_{UF} (mm)	Δp (kPa)	A_{UF} (m ²)	R (%)	E_T (-)
14	3	300	2.0	94	0.69
14	3	500	0.4	98	0.69
14	5	300	0.2	99	0.70
14	5	500	<0.01	>99	0.70
14	8	300	8.8	73	0.71
14	8	500	7.3	72	0.71
11	5	300	4.3	87	0.76
11	5	500	2.8	89	0.76
8	3	300	2.6	92	0.74
8	3	500	2.6	90	0.74
8	5	300	11.5	64	0.83
8	5	500	9	66	0.83
8	8	300	31.6	2	0.94
8	8	500	25	5	0.94

5. Conclusions

In this study, a process comprising particle classification and filtration was investigated by using a hydrocyclone and a pressure filter. The most novel part of the study was the evaluation of the pressure filtration properties of the produced underflow and overflow streams, and comparison of the filterability with respect to the required filtration area. According to the results of the hydrocyclone experiments, changes in the diameter of the underflow spigot had a more significant effect on the particle size (D_x) values than that of the vortex finder. The average specific cake resistances were higher for the overflow streams and lower for the underflow streams, compared to those of the feed slurry. Correspondingly, the average porosities of the filter cakes formed from the underflow streams were higher than those of the cakes formed from the feed slurry. When the width of particle size distribution increased the porosity of underflow cakes decreased. The pressure dependency of the feed and underflow cakes porosities indicated that the cakes were slightly compressible. The presence of fines in the slurries turned out to be the main reason for the weak predictability with the Kozeny-Carman equation: the results showed clearly that the fraction of very fine ($< 1 \mu\text{m}$) particles was the dominating factor affecting the specific cake resistance. Estimation of the filtration area required to produce ten tons of dry solids per hour showed that the required area for the underflow slurries was small in most cases, compared to the area required for overflow filtration. Due to the superior filterability of the dense underflows, the area requirement for the non-classified slurry was higher than the total area required for the filtration of the overflow and underflow streams in most experiments. By filtering only the underflow streams to recover solids, the required filtration areas could be reduced as much as by 99 %. These findings suggest that, besides efficient classification, hydrocyclones have a great potential in improving the filtration properties of slurries.

References

- Allen, T., 2003. Powder Sampling and Particle Size Determination. Elsevier B.V.
- Anlauf, H., Sorrentino, J.A., 2004. The Influence of Particle Collective Characteristics on Cake Filtration Results. Chem. Eng. Technol. 27(10), 1080-1084.
- Besra, L., Sengupta, D.K., Roy, S.K., 2000. Particle characteristics and their influence on dewatering of kaolin, calcite and quartz suspensions. Int. J. Miner.Process. 59, 89-112.
- Boylu, F., Cinku, K., Enseli, F., Celik, M.S., 2010. The separation efficiency of Na-bentonite by hydrocyclone and characterization of hydrocyclone products. Int. J. Miner. Process. 94, 196-202.
- Bradley, D., 1965. The Hydrocyclone. Pergamon Press.
- Braun, T., Bohnet, M., 1990. Influence of Feed Solids Concentration on the Performance of Hydrocyclones. Chem. Eng. Technol. 13(1), 1-20.
- Cilliers, J.J., 2000. Hydrocyclones for particle size separation. In: Encyclopedia of separation science, Eds. Poole C, Cooke M, Academic Press, UK.

Cilliers, J.J., Daiz-Anadon, L., Wee, F.S., 2004. Temperature, classification and dewatering in 10 mm hydrocyclones. *Miner. Eng.* 17, 591-597.

Cullivan, J.C., Williams, R.A., Dyakowski, T., Cross, C.R., 2004. New understanding of a hydrocyclone flow field and separation mechanism from computational fluid dynamics. *Miner. Eng.* 17, 651-660.

Darcy, H. P. G., 1856. *Les Fontaines Publiques de la Ville de Dijon*. Victor Dalamont, Paris.

Gao, S., Li, X., Wei, D., Fang, P., Jia, C., Liu, W., Han, C., 2008. Beneficiation of low-grade diasporic bauxite with hydrocyclone. *Trans. Nonferrous Met. Soc. China* 18, 444-448.

Ghadirian, M., Afacan, A., Hayes, R.E., Mmbaga, J.P., Mahmood, T., Xu, Z., Masliyah, J., 2015. A study of the hydrocyclone for the separation of light and heavy particles in aqueous slurry. *The Can. J. Chem. Eng.* 93, September 2015, 1667-1677.

Golmaei, M., Kinnarinen, T., Jernström, E., Häkkinen, A., 2018. Efficient separation of hazardous trace metals and improvement of the filtration properties of green liquor dregs by a hydrocyclone. *Journal of Cleaner production*. 183, 162-171.

Hogg, R., 2000. Flocculation and dewatering. *Int. J. Miner. Process.* 58, 223-236.

Hwang, K.-J., Chou, S.-J., 2017. Designing vortex finder structure for improving the particle separation efficiency of a hydrocyclone. *Sep. Purif. Technol.* 172, 76-84.

Kawatra, S.K., Bakshi, A.K., Rusesky, M.T., 1996. The effect of slurry viscosity on hydrocyclone classification. *Int. J. Miner. Process.* 48, 39-50.

Kinnarinen, T., Tuunila, R., Huhtanen, M., Häkkinen, A., Kejik, P., Sverak, T., 2015. Wet grinding of CaCO₃ with a stirred media mill: Influence of obtained particle size distributions on pressure filtration properties. *Powdr Technol.* 273, 54-61.

Kinnarinen, T., Tuunila, R., Häkkinen, A., 2017. Reduction of the width of particle size distribution to improve pressure filtration properties of slurries. *Miner. Eng.* 102, 68-74.

Lee, J., 2014. Separation of fine particles by a low-pressure hydrocyclone (LPH). *Aquacult. Eng.* 63, 32-38.

Mota, M., Teixeira, J.A., Bowen, W.R., Welshin, A., 2003. Interference of coarse and fine particles of different shape in mixed porous beds and filter cakes. *Miner. Eng.* 16, 135-144.

Neesse, Th., Dueck, J., 2007. Dynamic modelling of the hydrocyclone. *Miner. Eng.* 20, 380-386.

Neesse, Th., Dueck, J., Minkow, L., 2004a. Separation of finest particles in hydrocyclones. *Miner. Eng.* 17, 689-696.

Neesse, Th., Schneider, M., Golyk, V., Tiefel, H., 2004b. Measuring the operating state of the hydrocyclone. *Miner. Eng.* 17, 697-703.

Nowakowski, A.F., Cullivan, J.C., Williams, R.A., Dyakowski, T., 2004. Application of CFD to modelling of the flow in hydrocyclones. Is this a realizable option or still a research challenge? *Miner. Eng.* 17, 661-669.

Pasquier, S., Cilliers, J.J., 2000. Sub-micron particle dewatering using hydrocyclones. *Chem. Eng. J.* 80, 283-288.

Rhodes, M. J., 2008. *Introduction to particle technology*, 2nd Ed. John Wiley & Sons Ltd., Chichester, England.

Rushton, A., Ward, W.S., Holdich, R.G., 2000. *Solid-Liquid Filtration and Separation Technology*. 2nd Ed. Wiley-VCH, Weinheim.

Schuetz, S., Mayer, G., Bierdel, M., Piesche, M., 2004. Investigations on the flow and separation behaviour of hydrocyclones using computational fluid dynamics. *Int. J. Miner. Process.* 73, 229-237.

Svarovsky, L., 2000. *Solid-Liquid Separation*. 4th Ed.

Tien, C., Ramarao, B.V., 2013. Can filter cake porosity be estimated based on the Kozeny-Carman equation? *Powder Technology*. 237, 233-240.

Tavares, L.M., Souza, L.L.G., Lima, J.R.B., Possa, M.V., 2002. Modeling classification in small-diameter hydrocyclones under variable rheological conditions. *Miner. Eng.* 15, 613-622.

Wakeman, R., 2007. The influence of particle properties on filtration. *Sep. Purif. Technol.* 58, 234-241.

Yianatos, J.B., Lisboa, M.A., Baeza, D.R., 2002. Grinding capacity enhancement by solid concentration control of hydrocyclone underflow. *Miner. Eng.* 15, 317-323.

Yu, J.-F., Fu, J., Cheng, H., Cui, Z., 2017. Recycling of rare earth particle by mini-hydrocyclones. *Waste Management*. 61, 362-371.